High-Power Copper Gratings for a Sheet-Beam Traveling-Wave Amplifier at G-band

Colin D. Joye, *Member, IEEE*, Jeffrey P. Calame, *Senior Member, IEEE*, Alan M. Cook, *Member, IEEE*, and Morag Garven

***Abstract*—The design, fabrication, and electromagnetic cold testing results of an all-copper grating circuit intended for a G-band sheet-beam traveling-wave amplifier are presented. Fabrication was carried out via ultraviolet photolithography (UV-LIGA) using the SU-8 photoresists. Two cold test methods used to characterize the microfabricated circuits are reported and reveal excellent agreement with simulations. This type of all-copper grating also shows potential for use as a high-average-power sharp-cutoff filter.**

***Index Terms*—Copper grating, millimeter-wave (mmW) amplifiers, photolithography, slow-wave structures.**

I. Introduction

MICROFABRICATION techniques have become an increasingly crucial facet of the realization of millimeter-wave (mmW) and sub-mmW vacuum electron devices (VEDs) in recent years [1]–[5]. Compact, high-power, and high-gain VED sources with moderate bandwidth are useful for applications such as imaging [6], [7] and high-data-rate communications [8]. The sheet-beam concept promises to enhance the high-power capability of slow-wave VEDs by providing total beam current greater than that possible with a round beam [9]. The combination of the sheet-beam technology with planar microfabrication techniques is a natural pairing that lends itself to opportunities for VEDs.

Slow-wave amplifiers are very compact due to their intrinsically small electromagnetic circuit features, but these small features pose significant challenges for high-power generation because of the high thermal loading. Copper is among the best materials for vacuum compatibility, high-power-handling capability, and low microwave loss; hence, a technique has been developed for accurately microfabricating these mmW and sub-mmW structures from oxygen-free high-conductivity (OFHC) copper.

Fig. 1 shows the geometry of an amplifier based on a simple grating [5]. The sheet electron beam is guided over the microfabricated grating via an external magnetic field (not shown). A cover incorporating a shallow beam tunnel channel completes the interaction circuit. This circuit type, although inherently narrow band at low voltage, was chosen as a prototypical structure in order to develop UV-LIGA techniques that could be extended to more complex wideband high-power devices.

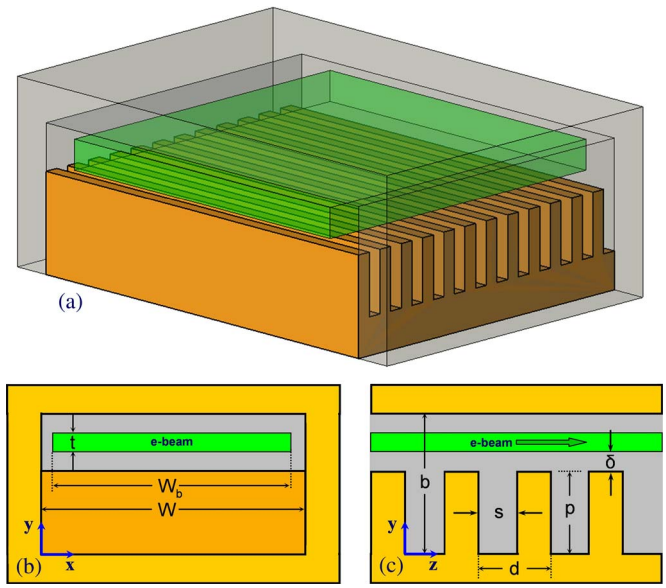

Fig. 1. Grating amplifier geometry in (a) perspective view, (b) front view, and (c) side view, with design variables and axes indicated.

II. Grating Amplifier Design

The complex dispersion relation can be used to estimate the gain of the amplifier by tracing roots with complex wavenumber k_z [10]. From the spatially growing root, along with the parameters listed in Table I, a peak linear growth rate of 33 dB $\cdot$ cm^{-1} is estimated at 211.3 GHz for the as-built circuit excluding losses. In the linear regime, the predicted frequency response with a -3-dB bandwidth is 0.5 GHz [5].

The slot depth p is the primary control for the interaction frequency and is the most sensitive parameter at -0.56 GHz $\cdot$ μm^{-1}. The slot width s is also quite sensitive at -0.37 GHz $\cdot$ μm^{-1}. Other parameters are relatively insensitive for the tolerances that are achieved. The maximum vertical aspect ratio needed is $p/s \approx 5$, which is easily achievable using UV-LIGA [11].

Manuscript received September 19, 2012; revised October 12, 2012; accepted October 22, 2012. Date of publication November 26, 2012; date of current version December 19, 2012. This work was supported by the U.S. Office of Naval Research. The review of this brief was arranged by Editor R. Carter.

C. D. Joye, J. P. Calame, and A. M. Cook are with the U.S. Naval Research Laboratory, Washington, DC 20375 USA (e-mail: colin.joye@nrl.navy.mil; jeffrey.calame@nrl.navy.mil; alan.cook@nrl.navy.mil).

M. Garven is with Science Applications International Corporation, McLean, VA 22102 USA (e-mail: Morag.Garven@nrl.navy.mil).

Color versions of one or more of the figures in this brief are available online at http://ieeexplore.ieee.org.

Digital Object Identifier 10.1109/TED.2012.2226591

TABLE I
220-GHz GRATING PARAMETERS

Parameter	Sym.	Target	As Fab'd
Grating period	d	150 μm	150 μm
Slot width	s	75 μm	81 μm avg
Slot depth	p	315 μm	313 μm ± 3
Number of slots	N	134	134
Beam tunnel	b-p	250 μm	250 μm ± 10
Grating width	W	2.2 mm	2.2 mm
Beam Width	W_b	1.8 mm	-
Beam thickness	t	160 μm	-
Beam voltage	V_0	19 kV	-
Beam current	I_0	0.5 A	-

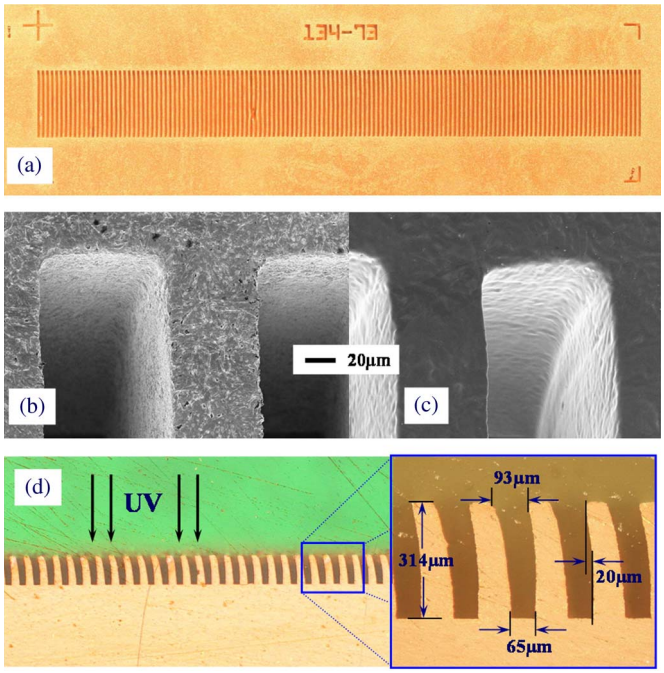

Fig. 2. (a) Completed G-band amplifier grating after SU-8 removal and cleaning. SEM images (b) before and (c) after annealing the grating at 950 °C in a hydrogen furnace. (d) Side view of a potted and sawn grating.

III. SU-8 PHOTOLITHOGRAPHY

Ultraviolet (UV) lithography is a microfabrication process that allows features down to just a few micrometers or even less to be fabricated using an inexpensive UV source. The SU-8 photoresist was chosen because of its very high viscosity, ability to be coated in extremely thick layers over 1 mm, and demonstrated capability for high aspect ratios and fine features [2], [11], [12]. Custom photolithography masks were purchased according to the specifications in Table I. The details of the UV-LIGA processes for forming of the negative SU-8 molds and for electroforming of copper are described in detail in [2]. Once the SU-8 molds are formed on a copper substrate, copper is then electroformed around the molds, ground to thickness, and polished. The SU-8 is removed by a molten salt process, followed by annealing in dry hydrogen.

Fig. 2 shows the optical images and scanning electron microscopy (SEM) images of the grating before and after it was annealed at 950 °C in a hydrogen furnace. The annealing sinters down the grain roughness on the surface, improving conductivity. The structures themselves do not deform in a significant way during the annealing process. Fig. 2(d) shows another grating from the same wafer that was potted in epoxy and sawn to view the side profile of the slots. Here, slight deformation of the fragile copper vanes, caused by excessively coarse sandpaper grinding, can be seen.

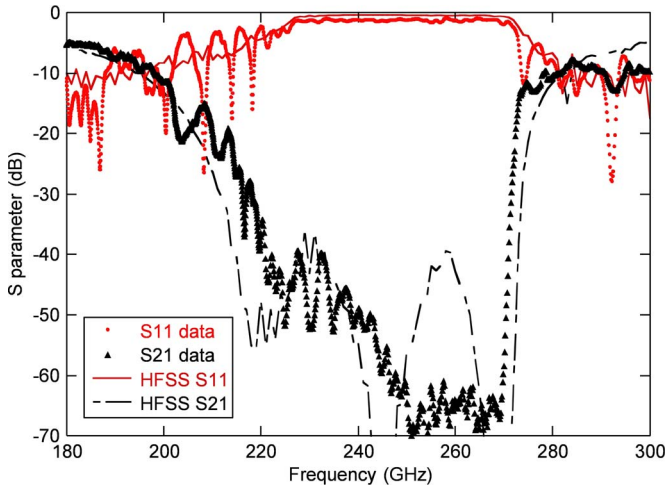

Fig. 3. Summary of cold test results for the grating showing (red circles) S_{11} and (black triangles) S_{21} along with (solid and dashed lines) HFSS simulations. The measurements show a very clear stopband with a sharp rise around 272 GHz [5].

IV. COLD TEST

The cold test is an important part of verifying the design and fabrication steps. The grating circuits were characterized electromagnetically in two ways: using a two-port cold test fixture (CTF) to measure both reflection and transmission over the grating and using a fixture incorporating a short over a portion of the grating to measure the dispersion relation directly. An Agilent E8364B vector network analyzer with extenders from OML, Inc., was used for measurements at W-, G-, and H-bands (75–110, 140–220, and 220–325 GHz, respectively).

A. Two-Port CTF

The CTF was CNC machined from OFHC copper. The gratings were tightly clamped into place in the fixture. The results of the cold test are shown in Fig. 3 and show good agreement with those of HFSS simulations. The two-port device produced a clean S_{11} signal of approximately -1.3 dB at the stopband between 225 and 272 GHz, demonstrating the low-loss capability of this all-copper device. The upper knee frequency of 272 GHz for the S_{21} measurement is a bit higher than the target value of 270 GHz. This can be traced to a slight taper in the beam tunnel height $\boldsymbol{b}$ over the length of the fixture, which directly alters only the upper knee frequency. Table II compares the two-port CTF to simulation, where the stopband covers the frequency range $\boldsymbol{f_1}$–$\boldsymbol{f_2}$.

The S_{21} measurement of the grating shown in Fig. 3 reveals a very deep stopband down to -70 dB (the noise floor), indicating that the grating has strong filtering capability with a regular

TABLE II
GRATING CTF COMPARISON

Param.	Simulation	2-port CTF	Target
b	230 μm	239 to 263 μm	250 μm
f_1	215 ± 0.5 GHz	212 ± 2 GHz	221 GHz
f_2	275 ± 0.2	272 ± 0.5	270 GHz

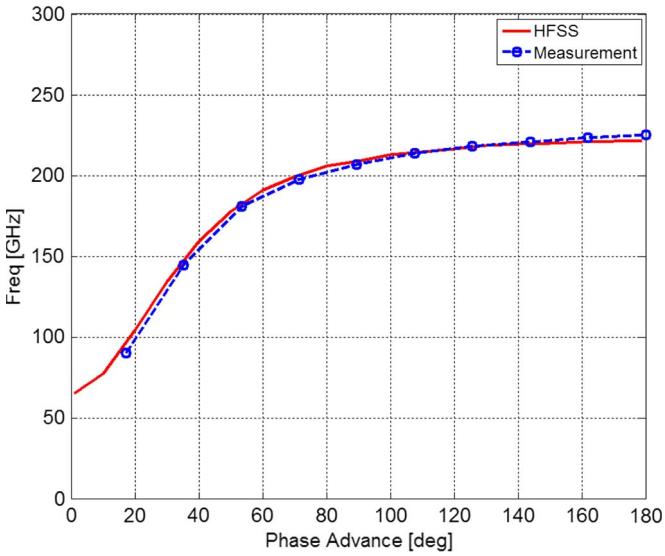

Fig. 4. Comparison of the (circles and dashed line) measured dispersion relation to the (solid line) as-built model simulated in HFSS.

periodicity. At around 270 GHz, the filter S_{21} transmission swings very sharply by 40 dB over just 2.5 GHz (0.93% BW) and spans 54 dB over 4.3 GHz (1.6% BW). Such a sharp rise points to possible use as a high-average-power filter with sharp cutoff for the upper-mmW range and beyond.

At 211.3 GHz, the operating frequency of the as-built device including beam loading effects, the measured losses in the circuit add up to 23.5 dB over 2 cm (Fig. 3). It is well known that the amplifier gain is reduced by only one-third of the total cold circuit loss, resulting in a total linear spatial growth rate of about 30 dB · cm^{-1}, excluding launching losses [13].

B. Shorted CTF

In order to directly measure the dispersion relation, a second CTF was CNC machined such that only ten slots were exposed, followed by a short for the rest of the grating. Adaptors to standard WR5 and WR10 waveguides were fabricated so that the structure could be tested at W-, G-, and H-bands to capture all of the relevant information. The results of the measurement, shown in Fig. 4, are in excellent agreement with those of the HFSS simulations that include the distortions in the slots, showing that the grating is tolerant to some types of nonideal slot profiles.

V. CONCLUSION AND FUTURE WORK

In summary, microfabrication and cold testing of gratings for vacuum electronics in the mmW regime have been demonstrated. Low-loss copper circuits with vertical aspect ratios up to 5 : 1 and feature sizes down to tens of micrometers have been fabricated using UV-LIGA techniques.

Investigations involving more complicated slow-wave structures fabricated using multiple-layer lithography will be performed. We are currently testing the microfabrication process at W-band through 670 GHz. The work described here, together with the ongoing process enhancements, will enable the fabrication and demonstration of new types of mmW and sub-mmW vacuum electronic amplifiers.

REFERENCES

[1] J. H. Booske, R. J. Dobbs, C. D. Joye, C. L. Kory, G. R. Neil, G. S. Park, J. H. Park, and R. J. Temkin, "Vacuum electronic high power terahertz sources," *IEEE Trans. Terahertz Sci. Technol.*, vol. 1, no. 1, pp. 54–75, Sep. 2011.

[2] C. D. Joye, J. P. Calame, M. Garven, and B. Levush, "UV-LIGA microfabrication of 220 GHz sheet beam amplifier gratings with SU-8 photoresist," *J. Micromech. Microeng.*, vol. 20, no. 12, p. 125 016, Dec. 2010.

[3] Y.-M. Shin, D. Gamzina, L. R. Barnett, F. Yaghmaie, A. Baig, and N. C. Luhmann, "UV lithography and molding fabrication of ultra-thick micrometallic structures using a KMPR photoresist," *J. Microelectromech. Syst.*, vol. 19, no. 3, pp. 683–689, Jun. 2010.

[4] S. J. Papadakis, J. A. Hoffmann, A. H. Monica, D. Deglau, J. Yu, T. Antonsen, G. Nusinovich, and R. Osiander, "A micro-fabricated sheet-beam Orotron THz source," in *Proc. SPIE, Conf. Micro–Nanotechnol. Sensors, Syst., Appl. III*, Orlando, FL, Apr. 25–29, 2011, p. 803 10C.

[5] C. D. Joye, J. P. Calame, K. Nguyen, D. Pershing, P. Larsen, M. Garven, D. Park, R. Bass, and B. Levush, "Microfabrication of wideband, distributed beam amplifiers at 220 GHz," in *Proc. IEEE Int. Vac. Electron. Conf.*, Bangalore, India, Feb. 21–24, 2011, pp. 343–344.

[6] M. A. Patrick, J. A. Holt, C. D. Joye, and F. C. De Lucia, "Elimination of speckle and target orientation requirements in millimeter-wave active imaging by modulated multimode mixing illumination," *J. Opt. Sci. Amer. A*, Jul. 2012.

[7] F. De Lucia, M. Patrick, J. Holt, and C. D. Joye, "Modulated multimode mixing illumination for the elimination of speckle and target orientation requirements in active imaging," in *Proc. USNC–URSI Conf.*, Boulder, CO, Jan. 5–7, 2012.

[8] J. Federici and L. Moeller, "Review of terahertz and subterahertz wireless communications," *J. Appl. Phys*, vol. 107, no. 11, p. 111 101, Jun. 2010.

[9] J. Pasour, K. Nguyen, E. Wright, A. Balkcum, J. Atkinson, M. Cusick, and B. Levush, "Demonstration of a 100-kW solenoidally focused sheet electron beam for millimeter-wave amplifiers," *IEEE Trans. Electron Devices*, vol. 58, no. 6, pp. 1792–1797, Jun. 2011.

[10] J. Joe, J. Scharer, J. Booske, and B. McVey, "Wave dispersion and growth analysis of low-voltage grating Cerenkov amplifiers," *Phys. Plasmas*, vol. 1, no. 1, pp. 176–188, Jan. 1994.

[11] C. D. Joye, J. P. Calame, K. T. Nguyen, and M. Garven, "Microfabrication of fine electron beam tunnels using UV-LIGA and embedded polymer monofilaments for vacuum electron devices," *J. Micromech. Microeng.*, vol. 22, no. 1, p. 015010, Jan. 2012.

[12] A. del Campo and C. Greiner, "SU-8: A photoresist for high-aspect-ratio and 3D photolithography," *J. Micromech. Microeng.*, vol. 17, no. 6, pp. R81–R95, Jun. 2007.

[13] J. R. Pierce, "Theory of beam-type traveling-wave tube," *Proc. IRE*, vol. 35, no. 2, pp. 111–123, Feb. 1947.

Colin D. Joye (M'03) received the Ph.D. degree from Massachusetts Institute of Technology, Cambridge, in 2008.

Since 2008, he has been with the Vacuum Electronics Branch, U.S. Naval Research Laboratory, Washington, DC.

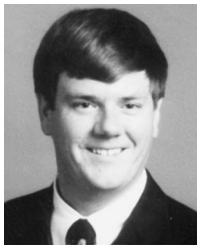

Jeffrey P. Calame (M'96–SM'11) received the Ph.D. degree in electrical engineering from the University of Maryland, College Park, in 1991.

Since 1997, he has been with the U.S. Naval Research Laboratory, Washington, DC.

Alan M. Cook (M'07) received the Ph.D. degree from the University of California, Los Angeles.

Since 2011, he has been with the U.S. Naval Research Laboratory, Washington, DC. His interests include millimeter wave and terahertz vacuum electron devices.

Morag Garven received the B.Sc. (with honors) and Ph.D. degrees from the University of Strathclyde, Glasgow, U.K., in 1989 and 1994, respectively.

She is currently under contract with Science Applications International Corporation, McLean, VA.